Robust Ultrashort Light Bullets in Strongly Twisted Waveguide Arrays

Carles Milián,[1,2,*] Yaroslav V. Kartashov,[1,3] and Lluis Torner[1,4]
[1]ICFO—Institut de Ciencies Fotoniques, The Barcelona Institute of Science and Technology, 08860 Castelldefels (Barcelona), Spain
[2]Institut Universitari de Matemàtica Pura i Aplicada, Universitat Politècnica de València, 46022 (València), Spain
[3]Institute of Spectroscopy, Russian Academy of Sciences, Troitsk, Moscow, 108840, Russia
[4]Universitat Politècnica de Catalunya, 08034 Barcelona, Spain

(Received 5 July 2019; published 27 September 2019)

We introduce a new class of stable light bullets that form in twisted waveguide arrays pumped with ultrashort pulses, where twisting offers a powerful knob to tune the properties of localized states. We find that, above a critical twist, three-dimensional wave packets are unambiguously stabilized, with no minimum energy threshold. As a consequence, when the higher-order perturbations that accompany ultrashort pulse propagation are at play, the bullets dynamically adjust and sweep along stable branches. Therefore, they are predicted to feature an unprecedented experimental robustness.

DOI: 10.1103/PhysRevLett.123.133902

The introduction by Silberberg several decades ago of the concept of *light bullets* [1], as self-trapped spatiotemporal wave packets of light, triggered intense research activity (see [2,3], and references therein). However, to date, their experimental observation in steady state form is still an essentially open challenge. Three-dimensional stable states were known to exist, even at that time, in several mathematical models [4], including parametric mixing in quadratic nonlinear media [5], and have been subsequently studied in media with saturable [6], competing [7,8], and nonlocal [9–11] nonlinearities, as well as in dissipative systems [12–17]. Stable light bullets were predicted to form in discrete [18,19] and continuous [20,21] lattices, too, even when carrying vorticity [22–24]. Experimentally, landmark advances were achieved when fundamental [25,26] and weakly unstable vortex [27] light bullets were observed to form, albeit in a transient regime, in photonic crystal fibers with periodic cores and, later, when nonlinearity-induced locking of relatively long pulses in different modes, resulting in the formation of spatiotemporal localized wave packets, was observed in graded-index media [28].

Nevertheless, despite the intense efforts conducted during the past two decades that have led to several different theoretical proposals for the existence of stable light bullets (see, also, the recent review [29]), their experimental observation over long distances remains elusive [25–27]. One of the salient challenges arises from the presence of *higher-order effects* (HOEs) that may destroy the bullet states existing in reduced mathematical models, where HOEs are disregarded. In practice, however, HOEs are actually significant and, thus, play an important role in experiments conducted with the ultrashort (subpicosecond) pump pulses that are required in order to generate enough group-velocity dispersion for a spatiotemporal state to form over many dispersion lengths. As a consequence, to date, the experimental formation of long-lived bullets has not been achieved.

In this Letter, we report on the existence of stable light bullets that are predicted to be observable as robust three-dimensional wave packets for unprecedented propagation distances even in the presence of HOEs. We found such states in twisted waveguide arrays, otherwise known to support stable spatial solitons [30–32]. Here we limit ourselves to bullets at the corners of square arrays, where centrifugal effects, key to our prediction, are maximal [32], but our results can be extended to triangular or hexagonal geometries. It is important to realize that the centrifugal effects lead to the qualitative modification of the bullet properties, contrasting with the properties of bullets at the interfaces of static arrays [33] (or, in order words, three-dimensional generalizations of corner solitons [34,35]). Twisting offers a unique tunability knob for the existence, stability, and localization of three-dimensional states, which is not available for other types of array modulations [36,37]. At low twist rates, we found two separate stability domains that, above a critical twist rate, merge into a single stability domain extending up to zero energy. Therefore, the energy threshold for stability vanishes and self-trapped three-dimensional states can remain stable even in the presence of continuous energy leakage due to small perturbations. This is in contrast to the abrupt bullet disintegration predicted to occur, e.g., in straight arrays when the energy carried by the bullet drops below the corresponding threshold.

We address square waveguide arrays with a constant twist rate around their center [cf. Fig. 1(a)]. Such arrays can be realized in doped silica fibers [38], where twists can be readily applied [39]. We analyze both truncated (without HOEs) and full (with HOEs) propagation regimes of

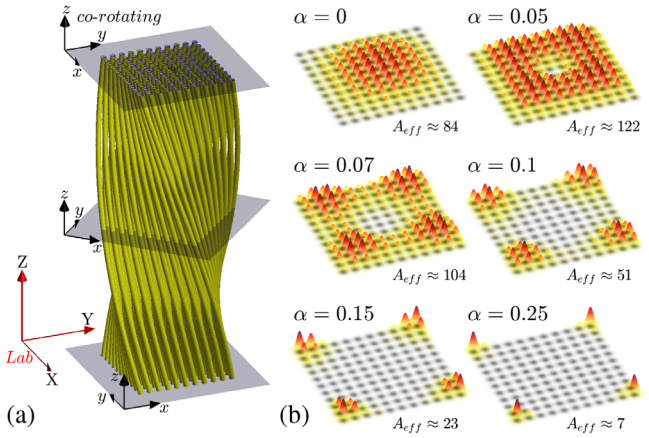

FIG. 1. (a) Twisted array of 11×11 waveguides. Axes are shown in the laboratory (red) and corotating (black) frames. (b) Amplitude profiles of the fundamental mode and effective mode area for different twist rates α. The gray background shows the potential cross section with $p = 12$, $d = 1.5$, and $w = 0.5$ [see the definition of parameters below Eq. (1)].

spatiotemporal wave packets along the z axis. Under paraxial and slowly varying envelope approximations, the evolution of linearly polarized light is governed by the dimensionless nonlinear Schrödinger equation:

$$i\partial_z\psi = -\frac{1}{2}\Delta\psi + i\alpha(x\partial_y - y\partial_x)\psi - (V + |\psi|^2)\psi - \mathcal{P}. \qquad (1)$$

$\Delta \equiv \partial_x^2 + \partial_y^2 + \partial_t^2$, $x = [X\cos(\alpha z) + Y\sin(\alpha z)]/w_0$, and $y = [Y\cos(\alpha z) - X\sin(\alpha z)]/w_0$ are the scaled transverse coordinates in the corotating frame [Fig. 1(a)] with rate $\alpha \equiv 2\pi/z_h$, $z \equiv Z/Z_R$ is the normalized propagation distance, $Z_R \equiv k_0 n_0 w_0^2$ is the diffraction length, w_0 is a reference width, $k_0 = \omega_0/c$, ω_0 is the carrier frequency, n_0 is the unperturbed refractive index defining the dispersion $\kappa(\omega) \equiv n_0(\omega)\omega/c$, $t = (T - Z/v_g)/T_s$ is the time in the frame moving with group velocity v_g, $T_s \equiv w_0[-\kappa^{(2)}\kappa(\omega_0)]^{1/2}$ is the time scaling, $\kappa^{(2)} \equiv \partial_\omega^2\kappa(\omega_0) < 0$ is the anomalous group velocity dispersion coefficient, $I = |\psi|^2/[k_0 Z_R n_2]$ is the intensity, and n_2 is the nonlinear index. For a square array of N^2 waveguides, the potential $V = p\sum_{m,n=1}^{N}\exp\{-[(x - x_m)^2 + (y - y_n)^2]/w^2\}$, where (x_m, y_n) are nodes of the grid with period d and $p = (k_0 w_0)^2 n_0 \delta n_{\max}$, where $\delta n = n - n_0$. Our model accounts for radiation leakage in contrast to discrete models [18,19,33], particularly important for the dynamical tests of bullet robustness (cf. Fig. 5), which may be affected by continuum modes. The function $\mathcal{P}$ accounts for the HOEs, described below in Eq. (2).

An important feature of the system resides in its linear spectrum. By increasing the twist, the fundamental mode is expelled from the center [Fig. 1(b)] and localized around the corners due to the effective Coriolis force $\sim\alpha$ [30,32,40]. Above $\alpha \approx 0.05$, the effective mode area $A_{\text{eff}} \equiv [\iint_{-\infty}^{+\infty}|\phi|^2 dxdy]^2/\iint_{-\infty}^{+\infty}|\phi|^4 dxdy$ decreases monotonically with α (see below).

We obtained three-dimensional stationary solutions of Eq. (1) without HOEs, $\psi = u(x, y, t)e^{ibz}$, using a modified square operator method [41]. Figure 2(a) shows the energy $U \equiv \iiint_{-\infty}^{+\infty}|u|^2 dxdydt$ versus b for bullet families located at one corner of the array with various twist rates α. We checked that bullets located at the center of the array are

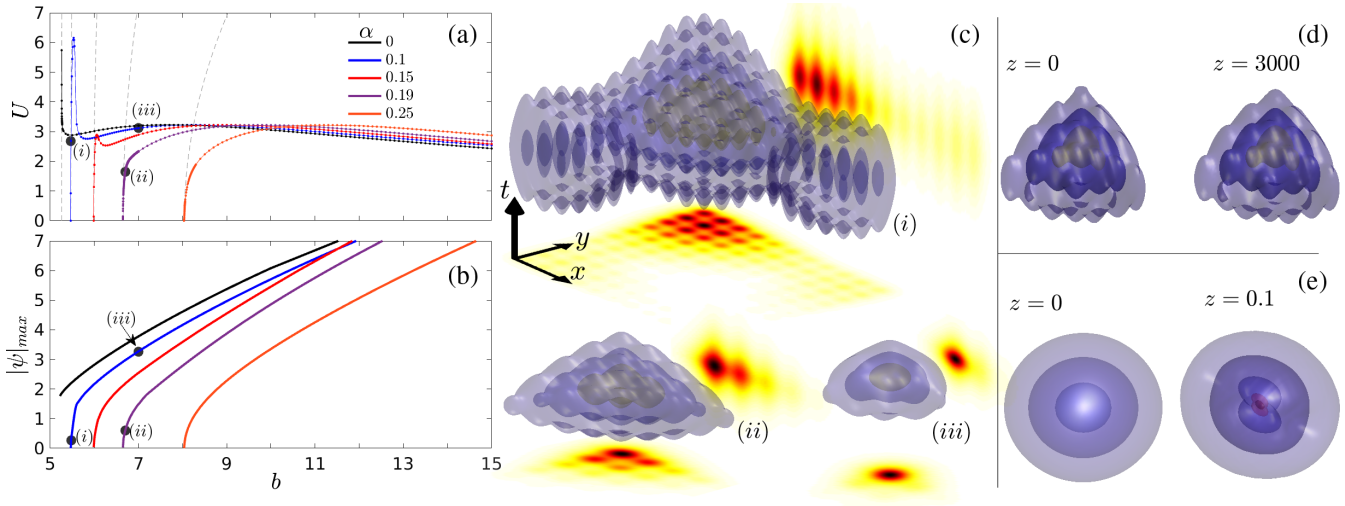

FIG. 2. (a) Energy and (b) peak amplitude of bullets versus the propagation constant for several twist rates (see the legend) in the array depicted in Fig. 1. (c) Stationary bullets corresponding to dots (i)–(iii) in (a) and (b). The 2D projections show profiles in the xt and xy planes. (d),(e) show the input (left) and output (right) of propagation with Eq. (1) initiated with (d) stable [$\alpha = 0.15$, $b = 6.4$] and (e) unstable [$\alpha = 0.15$, $b = 12$] solutions. The 3D contours are taken at 1/10, 1/100, and 1/1000 (c),(d) and at 1/2, 1/4, 1/10, 1/20, and 1/40 (e) of the maximum amplitude. The two inner red contours at $z = 0.1$ in (e) show high-intensity regions due to collapse at the bullet center.

almost insensitive to twist (not shown). Without twist ($\alpha = 0$), families of bullets localized at the center or corner channels share the same qualitative features in terms of $U(b)$ curves; hence a comparison with Ref. [20] is possible. The stability of light bullets, checked via extensive propagation simulations [see Figs. 2(d) and 2(e)], coincides well with the Vakhitov-Kolokolov (VK) criterion [42] predicting stability for $\partial_b U > 0$ and instability otherwise. At low twist rates $\alpha \lesssim 0.17$, the $U(b)$ curves exhibit two stable regions. The stability domain on the right of the plot is equivalent to the stability domain reported for static arrays ($\alpha = 0$) [20,43]. The stability domain on the left, at lower b values, extends up to arbitrarily small energies $U \to 0$ and terminates at the cutoff $b = b_{\rm co}$. In this linear limit, bullet amplitudes $|\psi|_{\rm max}$ vanish [Fig. 2(b)]. In the limit $\alpha \to 0$, the $U(b)$ curve features a strong peak for $b \to b_{\rm co}$, a reminiscence from free space [20,44,45]. When α increases, such a peak gradually disappears, leading to the merging of the two stability domains into a single domain at $\alpha \approx 0.17$.

In the limit $b \to b_{\rm co}$, bullets asymptotically transform into $\psi = \phi(x, y)A(z, t)e^{i(b_{\rm co}+\delta b)z}$, where ϕ is a linear mode of V, A is the temporal envelope, and δb is the propagation constant offset from the cutoff. Substituting the above ansatz into Eq. (1) and integrating the resulting equation for A, we get $U_{\rm co}(\delta b) \approx (8\delta b)^{1/2}A_{\rm eff}$. In contrast to unbound systems, where $A_{\rm eff} \to \infty$ causes $U_{\rm co}$ to diverge [44,45], in the finite array $A_{\rm eff}$ is finite, and, thus, $U(b_{\rm co}) \equiv 0$ as $\delta b \to 0$. Moreover, a monotonic decrease of $A_{\rm eff}$ with twist [see Fig. 1(b)] results in a considerable decrease of the slope $\partial_b U|_{b_{\rm co}} = (2/b)^{1/2}A_{\rm eff}$ near the cutoff, which is related to the merging of stable regions. This asymptotic trend is marked in Fig. 2(a) by light gray curves, in excellent agreement with the actual $U(b)$ curves around the cutoff. We verified that the localized corner modes also form in twisted arrays with random fluctuations ~3% [38,46] in channel positions and widths.

Figure 2(c) shows light bullets for $\alpha = 0.1$ [(i) and (iii)] and $\alpha = 0.19$ [(ii)]. Such bullets have noncanonical shapes—they are strongly asymmetric in space, because they are localized in the corners of the array due to the interplay of centrifugal force and refraction, in contrast to previously reported symmetric states forming in the center of an untwisted array. A new feature of such bullets is that, in addition to nonlinearity, their localization degree is strongly affected by the twist rate of the array. Note also that increasing the twist leads to stronger localization [cf. bullets (i) and (ii)], as it happens when increasing b [cf. bullets (i) and (iii)]. We checked the stability of the bullet solutions by long ($z = 3000$) three-dimensional propagation simulations initiated with stationary solutions perturbed with a 1% noise in the amplitude and phase. An illustrative stable evolution is shown in Fig. 2(d). Unstable states either decay or collapse. An example of the latter, that typically occurs for large b values, is shown in Fig. 2(e), where high intensities develop around the bullet center.

The transformation of the $U(b)$ curves with α [cf. Fig. 2(a)] is reflected in the Hamiltonian-energy diagrams shown in Fig. 3. The existence of cusps (see markers) corresponds to points where $\partial_b U = 0$ [Fig. 2(a)]. When α increases, the cusps move in the $H(U)$ plane, and two of them cease to exist for $\alpha \approx 0.17$ when a single stability region forms [cf. Fig. 2(a)]. In the $H(U)$ diagrams, the bullet branches emerging from the cutoff correspond to straight lines departing from the origin with slope $b_{\rm co}$. This is seen from the Hamiltonian of Eq. (1), $H \equiv \iiint_{-\infty}^{\infty} dxdydt\mathcal{H}$, $\mathcal{H} = {\rm Re}\{\psi^*[-\Delta/2 + i\alpha(x\partial_y - y\partial_x) - V - |\psi|^2]\psi\} + |\psi|^4/2$, which evaluated for a bullet reads $H = -bU + Q$ ($Q \equiv \iiint_{-\infty}^{\infty} dxdydt|\psi|^4/2$). Since Q decreases faster than U when $b \to b_{\rm co}$, this limit yields $U, H \to 0$ and $\partial_U H(b_{\rm co}) = b_{\rm co}$. For $\alpha = 0$, the cutoff cannot be reached numerically [43], but the linear spectrum suggests that the cusp marked with a diamond is located at $U \sim 100$, well outside the depicted area. Figure 3 depicts that twist impacts the shapes of the $H(U)$ diagrams strongly. Such shapes are important, because their cusps and minima reveal stability, instability, and metastability, as in many other systems [9,47,48].

Experimentally observable properties of the bullets are illustrated in Fig. 4, which shows bullet families as peak amplitude $|\psi|_{\rm max}$, energy U, and spatial width w_x versus temporal width w_t: $w_\xi \equiv [\iiint_{-\infty}^{+\infty}(\xi - \xi_0)^2|u|^2 dxdydt/U]^{1/2}$, where ξ denotes x or t and ξ_0 is evaluated at the bullet peak. The linear limit is at $w_t \to \infty$, where U, $|\psi|_{\rm max} \to 0$. The VK stable regions correspond to $\partial_{w_t} U < 0$.

Next, we address the robustness of the bullets in the presence of HOEs that enter into play in material systems

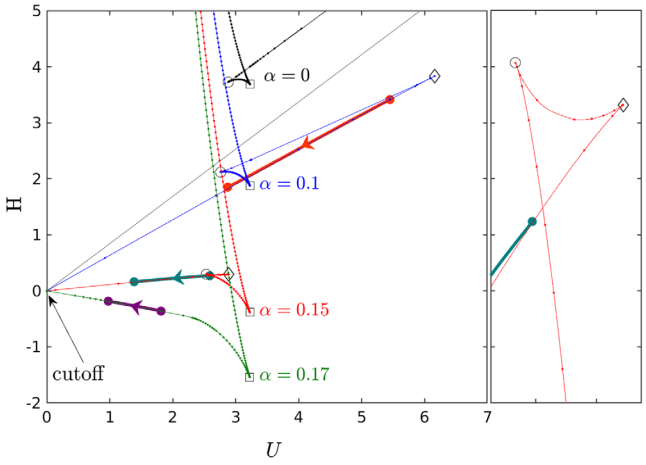

FIG. 3. Hamiltonian versus energy for bullet families with several values of α. For visual purposes, we plot the quantity $H \to H - {\rm const} \times U$ (with const $= -6.1$). The right panel enlarges around the swallowtail at $\alpha = 0.15$, and cusps are highlighted with markers. The thick traces with arrows mark the dynamical evolution of the bullets under HOEs [see the discussion after Eq. (2)]. Input or output values are marked with filled circles.

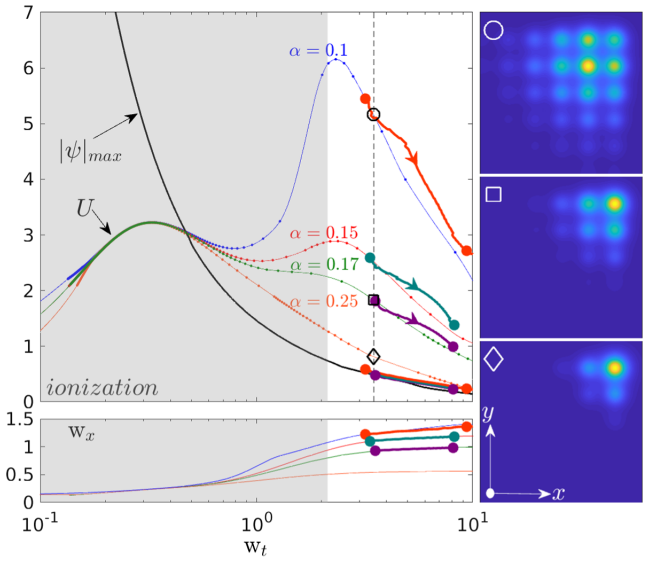

FIG. 4. Energy, amplitude, and spatial width of light bullet families versus the temporal width. The $|\psi|_{\max}(w_t)$ curves are very close to each other, and they are all well represented by the single black curve. The gray area ($w_t < 2.1$) marks the estimated ionization region in fused silica at $\lambda_0 = 1.55$ μm and scaling factor $T_s = 12$ fs. The insets show the bullet spatial cross sections with $w_t = 3.54$ for $\alpha = 0.1$, 0.17, and 0.25 (see markers in the main figure). The thick traces mark the evolution of U, $|\psi|_{\max}$, w_x, and w_t under the action of HOEs, corresponding to the traces in Fig. 3.

pumped with subpicosecond light pulses. In fused silica, the relevant HOEs are

$$\mathcal{P} \approx \frac{1}{|\kappa^{(2)}|}\sum_{q=3}^{\infty}\frac{\kappa^{(q)}}{T_s^{q-2}}\frac{(i\partial_t)^q}{q!}\psi + \frac{i\partial_\tau(|\psi|^2\psi)}{\omega_0 T_s} - \mu\psi\left(|\psi|^2 - \int_{-\infty}^{\infty} d\tau' |\psi(\tau-\tau')|^2 h_R(\tau')\right) + i\frac{b_K}{2}|\psi|^{2K-2}\psi \quad (2)$$

and account, respectively, for higher-order dispersion [49], self-steepening, Raman scattering, and multiphoton absorption (MPA): $\kappa^{(q)} \equiv \partial_\omega^q \kappa(\omega_0)$, $\mu = 0.18$, $h_R(\tau) = (\tau_1^2+\tau_2^2)/(\tau_1\tau_2^2)\theta(c\tau)\exp(-\tau/\tau_2)\sin(\tau/\tau_1)$, $\tau_1 = 12.2(\text{fs})/T_s$, $\tau_2 = 32\ (\text{fs})/T_s$, $\theta(\tau)$ is the Heaviside function, $b_K \equiv \beta_K Z_R/[k_0 n_2 Z_R]^{k-1}$, and $K \equiv \lfloor \hbar\omega_0/U_i + 1 \rfloor = 12$ ($\lfloor\cdot\rfloor$ denotes the floor function) is the number of simultaneously absorbed photons at the wavelength $\lambda_0 \sim 1.55$ μm, where $U_i \approx 9$ eV is the ionization potential [50]. Also, $\beta_K = 7.3 \times 10^{-169}$ m^{21}/W^{11} is the MPA coefficient, which accounts for ionization in the absence of impurities and light intensities well below the tunnel ionization regime (see, e.g., [51]). Obviously, we consider bullets at intensity levels well below the filamentation onset; thus MPA is negligible with respect to the Kerr effect, i.e., $[b_K|\psi|^{2K-2}/2]/|\psi|^2 \lesssim 10^{-5}$ [50–53]. For $w_0 = 30$ μm, the temporal scaling is $T_s = 12$ fs, the index contrast is $\delta n \approx 6 \times 10^{-4}$ ($p = 12$) in Ge-doped glass [54–56], $Z_R \approx 5$ mm, and $Z_h \approx 30$ cm (for $\alpha = 0.1$).

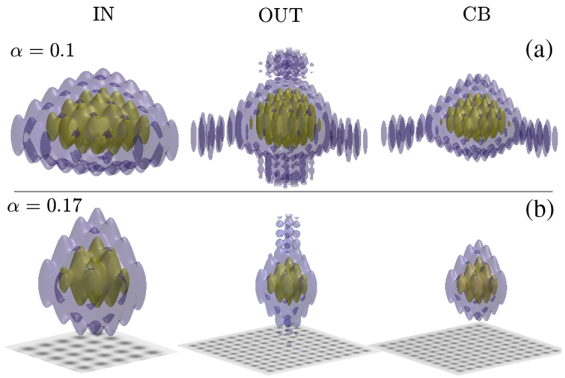

FIG. 5. Robust bullets with (a) $\alpha = 0.1$ and (b) $\alpha = 0.17$. The 3D contours show input ($z = 0$, left) and output ($z = 300$, middle) profiles. The rightmost column shows the stationary *corresponding bullet* (CB) to out profiles (see the text). (a) and (b) correspond to the orange and purple traces, respectively, in Figs. 3 and 4. A cross section of V is shown for reference; bullets are at the top corner.

To elucidate the robustness of the bullets, we propagated them numerically in the presence of all HOEs included in Eq. (2) over the distance $z = 300 \approx 1.55$ m $\approx 30 Z_d$, where $Z_d \equiv T_s^2 w_t^2/|\kappa^{(2)}|$ is the dispersion length and $\kappa^{(2)} \approx 28$ fs^2/mm. Illustrative input (IN) and output (OUT) profiles are shown in Fig. 5, in the left and middle columns. With the above scaling, input bullets have peak intensities of the order of 40 GW/cm^2. The corresponding variation of the bullet parameters (H, U, $|\psi|_{\max}$ w_x, and w_t) upon propagation is shown by the thick traces with arrows in Figs. 3 and 4. Over such propagation distances, bullets broaden from $w_t \approx 43$ fs to $\approx$120 fs. The traces show that the values of all parameters follow well those of the stationary bullet families; i.e., as HOEs are perturbative they smoothly transform a given bullet into a new one of the same stable family with lower U. The sweep along a family occurs because Raman and self-steepening break the global conservation of H and cause the fraction of total H and U carried by the bullets to vary [57,58], but solutions remain close to the stable $H(U)$ branch (Fig. 3). The emitted radiation is clearly seen in the output (OUT) profiles in Fig. 5 [middle column]. For completeness, we have added the right column showing the profile of the ideal stationary bullet with the same parameters as the output state (OUT). These profiles are termed *corresponding bullet* (CB) and are identical to those at the output (OUT), apart from the weak radiation.

In summary, we highlight that twisting fiber arrays affords a powerful physical mechanism to impact the properties of multidimensional wave packets, which we found to result in *stable three-dimensional light bullets*

without an energy threshold that exist, *above a critical twist*, as robust states localized at the corners of the array. Our results suggest that long-lived propagation of such light bullets should be experimentally feasible with ultrashort pump pulses and moderate peak powers. With a suitable design of the array and pump conditions, the bullet energy, peak amplitude, and widths (in space and time) can remain close to the values corresponding to the stationary solutions as bullets evolve in the presence of HOEs. Dynamical evolution where stable multidimensional solitons are stationary in the presence of HOEs was reported previously only in cavities (see, e.g., [12,59]). Here we found that a similar phenomenon occurs in single-pass twisted arrays. Our calculations were performed for the parameters of structured Ge-doped silica fibers that can be fabricated with lengths far exceeding the twist periods ~30 cm, with diffraction $\sim k_0 n_0 w_0^2 w_x^2$ and dispersion $\sim T_s^2 w_t^2/|\kappa^{(2)}|$ lengths of the order of centimeters, for pump pulses with FWHM ~ 50 fs. We assumed HOEs to remain perturbative, an assumption that we verified can hold in Ge-doped silica fibers under properly designed experimental conditions.

The work was supported by the Government of Spain through Juan de la Cierva Incorporación (IJCI-2016-27752), Severo Ochoa SEV-2015-0522, and FIS2015-71559-P; Generalitat de Catalunya; Centres de Recerca de Catalunya; Fundació Cellex; and Fundació Mir-Puig. C. M. thanks Professors J. Alberto Conejero Casares and Pedro Fernández de Córdoba Castellá for their support.

*carmien@upvnet.upv.es

[1] Y. Silberberg, Collapse of optical pulses, Opt. Lett. **15**, 1282 (1990).
[2] B. A. Malomed, D. Mihalache, F. Wise, and L. Torner, Spatiotemporal optical solitons, J. Opt. B **7**, R53 (2005).
[3] D. Mihalache, Linear and nonlinear light bullets: Recent theoretical and experimental studies, Rom. J. Phys. **57**, 352 (2012).
[4] E. A. Kuznetsov, A. M. Rubenchik, and V. E. Zakharov, Soliton stability in plasmas and hydrodynamics, Phys. Rep. **142**, 103 (1986).
[5] A. A. Kanashov and A. M. Rubenchik, On diffraction and dispersion effect on three wave interaction, Physica D (Amsterdam) **4D**, 122 (1981).
[6] D. E. Edmundson and R. H. Enns, Robust bistable light bullets, Opt. Lett. **17**, 586 (1992).
[7] A. Desyatnikov, A. Maimistov, and B. Malomed, Three-dimensional spinning solitons in dispersive media with the cubic-quintic nonlinearity, Phys. Rev. E **61**, 3107 (2000).
[8] D. Mihalache, D. Mazilu, L.-C. Crasovan, I. Towers, A. V. Buryak, B. A. Malomed, L. Torner, J. P. Torres, and F. Lederer, Stable Spinning optical Solitons in Three Dimensions, Phys. Rev. Lett. **88**, 073902 (2002).
[9] O. Bang, W. Krolikowski, J. Wyller, and J. J. Rasmussen, Collapse arrest and soliton stabilization in nonlocal nonlinear media, Phys. Rev. E **66**, 046619 (2002).
[10] D. Mihalache, D. Mazilu, F. Lederer, B. A. Malomed, Y. V. Kartashov, L. C. Crasovan, and L. Torner, Three-dimensional spatiotemporal optical solitons in nonlocal nonlinear media, Phys. Rev. E **73**, 025601(R) (2006).
[11] I. B. Burgess, M. Peccianti, G. Assanto, and R. Morandotti, Accessible Light Bullets Via Synergetic Nonlinearities, Phys. Rev. Lett. **102**, 203903 (2009).
[12] M. Brambilla, T. Maggipinto, G. Patera, and L. Columbo, Cavity Light Bullets: Three-Dimensional Localized Structures in a Nonlinear Optical Resonator, Phys. Rev. Lett. **93**, 203901 (2004).
[13] P. Grelu, J. M. Soto-Crespo, and N. Akhmediev, Light bullets and dynamic pattern formation in nonlinear dissipative systems, Opt. Express **13**, 9352 (2005).
[14] V. Skarka and N. B. Aleksic, Stability Criterion for Dissipative soliton Solutions of the One-, Two-, and Three-Dimensional Complex Cubic-Quintic Ginzburg-Landau Equations, Phys. Rev. Lett. **96**, 013903 (2006).
[15] D. Mihalache, D. Mazilu, F. Lederer, Y. V. Kartashov, L. C. Crasovan, L. Torner, and B. A. Malomed, Stable Vortex Tori in the Three-Dimensional Cubic-Quintic Ginzburg-Landau Equation, Phys. Rev. Lett. **97**, 073904 (2006).
[16] N. A. Veretenov, N. N. Rosanov, and S. V. Fedorov, Rotating and Precessing Dissipative-Optical-Topological-3D Solitons, Phys. Rev. Lett. **117**, 183901 (2016).
[17] S. V. Fedorov, N. A. Veretenov, and N. N. Rosanov, Irreversible Hysteresis of Internal Structure of Tangle Dissipative Optical Solitons, Phys. Rev. Lett. **122**, 023903 (2019).
[18] A. B. Aceves, C. De Angelis, A. M. Rubenchik, and S. K. Turitsyn, Multidimensional solitons in fiber arrays, Opt. Lett. **19**, 329 (1994).
[19] A. B. Aceves, G. G. Luther, C. De Angelis, A. M. Rubenchik, and S. K. Turitsyn, Energy Localization in Nonlinear Fiber Arrays: Collapse-Effect Compressor, Phys. Rev. Lett. **75**, 73 (1995).
[20] D. Mihalache, D. Mazilu, F. Lederer, Y. V. Kartashov, L.-C. Crasovan, and L. Torner, Stable three-dimensional spatiotemporal solitons in a two-dimensional photonic lattice, Phys. Rev. E **70**, 055603(R) (2004).
[21] D. Mihalache, D. Mazilu, F. Lederer, B. A. Malomed, Y. V. Kartashov, L. C. Crasovan, and L. Torner, Stable Spatiotemporal Solitons in Bessel Optical Lattices, Phys. Rev. Lett. **95**, 023902 (2005).
[22] H. Leblond, B. A. Malomed, and D. Mihalache, Three-dimensional vortex solitons in quasi-two-dimensional lattices, Phys. Rev. E **76**, 026604 (2007).
[23] H. Leblond, B. A. Malomed, and D. Mihalache, Spatiotemporal vortex solitons in hexagonal arrays of waveguides, Phys. Rev. A **83**, 063825 (2011).
[24] D. Cheskis, S. Bar-Ad, R. Morandotti, J. S. Aitchison, H. S. Eisenberg, Y. Silberberg, and D. Ross, Strong Spatiotemporal Localization in a Silica Nonlinear Waveguide Array, Phys. Rev. Lett. **91**, 223901 (2003).
[25] S. Minardi, F. Eilenberger, Y. V. Kartashov, A. Szameit, U. Röpke, J. Kobelke, K. Schuster, H. Bartelt, S. Nolte, L. Torner, F. Lederer, A. Tünnermann, and T. Pertsch,

Three-Dimensional Light Bullets in Arrays of Waveguides, Phys. Rev. Lett. **105**, 263901 (2010).
[26] F. Eilenberger, S. Minardi, A. Szameit, U. Röpke, J. Kobelke, K. Schuster, H. Bartelt, S. Nolte, L. Torner, F. Lederer, A. Tünnermann, and T. Pertsch, Evolution dynamics of discrete-continuous light bullets, Phys. Rev. A **84**, 013836 (2011).
[27] F. Eilenberger, K. Prater, S. Minardi, R. Geiss, U. Röpke, J. Kobelke, K. Schuster, H. Bartelt, S. Nolte, A. Tünnermann, and T. Pertsch, Observation of Discrete, Vortex Light Bullets, Phys. Rev. X **3**, 041031 (2013).
[28] W. H. Renninger and F. W. Wise, Optical solitons in graded-index multimode fibres, Nat. Commun. **4**, 1719 (2013).
[29] Y. V. Kartashov, G. Astrakharchik, B. Malomed, and L. Torner, Frontiers in multidimensional self-trapping of nonlinear fields and matter, Nat. Rev. Phys. **1**, 185 (2019).
[30] H. Sakaguchi and B. A. Malomed, Solitary vortices and gap solitons in rotating optical lattices, Phys. Rev. A **79**, 043606 (2009).
[31] J. Cuevas, B. A. Malomed, and P. G. Kevrekidis, Two-dimensional discrete solitons in rotating lattices, Phys. Rev. E **76**, 046608 (2007).
[32] X. Zhang, F. Ye, Y. V. Kartashov, V. A. Vysloukh, and X. Chen, Localized waves supported by the rotating waveguide array, Opt. Lett. **41**, 4106 (2016).
[33] D. Mihalache, D. Mazilu, F. Lederer, and Y. S. Kivshar, Stable discrete surface light bullets, Opt. Express **15**, 589 (2007).
[34] K. G. Makris, J. Hudock, D. N. Christodoulides, G. I. Stegeman, O. Manela, and M. Segev, Surface lattice solitons, Opt. Lett. **31**, 2774 (2006).
[35] F. Lederer, G. I. Stegeman, D. N. Christodoulides, G. Assanto, M. Segev, and Y. Silberberg, Discrete solitons in optics, Phys. Rep. **463**, 1 (2008).
[36] V. E. Lobanov, Y. V. Kartashov, and L. Torner, Light Bullets by Synthetic Diffraction-Dispersion Matching, Phys. Rev. Lett. **105**, 033901 (2010).
[37] M. Matuszewski, I. L. Garanovich, and A. A. Sukhorukov, Light bullets in nonlinear periodically curved waveguide arrays, Phys. Rev. A **81**, 043833 (2010).
[38] H. K. Chandrasekharan, F. Izdebski, I. Gris-Sánchez, N. Krstajic, R. Walker, H. L. Bridle, P. A. Dalgarno, W. N. MacPherson, R. K. Henderson, T. A. Birks, and R. Thomson, Multiplexed single-mode wavelength-to-time mapping of multimode light, Nat. Commun. **8**, 14080 (2017).
[39] G. K. L. Wong, M. S. Kang, H. W. Lee, F. Biancalana, C. Conti, T. Weiss, and P. S. J. Russell, Excitation of Orbital Angular Momentum Resonances in Helically Twisted Photonic Crystal Fiber, Science **337**, 446 (2012).
[40] Y. V. Kartashov, V. A. Vysloukh, and L. Torner, Rotating surface solitons, Opt. Lett. **32**, 2948 (2007).
[41] J. Yang, *Nonlinear Waves in Integrable and Nonintegrable Systems* (SIAM, Philadelphia, 2010), ISBN 978-0-89871-705-1.
[42] N. G. Vakhitov and A. A. Kolokolov, Stationary solutions of the wave equation in a medium with nonlinearity saturation, Radiophys. Quantum Electron. **16**, 783 (1973).
[43] The thresholdless stability regions shown in Fig. 2(a) are extremely sharply peaked for small twist values $\alpha \ll 0.1$, and they become technically difficult to be numerically explored. This is presumably why this very relevant feature, in principle general for any truncated system, has not been reported in the previous numerical studies. In the current work, our numerical method was incapable of tracing the $U(b)$ down to the cutoff for $\alpha = 0$.
[44] Y. S. Kivshar and G. P. Agrawal, *Optical Solitons: From Fibers to Photonic Crystals* (Academic, San Diego, 2003).
[45] N. N. Akhmediev and A. Ankiewicz, *Solitons: Nonlinear Pulses and Beams* (Chapman and Hall, London, 1997).
[46] P. J. Mosley, I. Gris-Sánchez, J. M. Stone, R. J. A. Francis-Jones, D. J. Ashton, and T. A. Birks, Characterizing the variation of propagation constants in multicore fiber, Opt. Express **22**, 25689 (2014).
[47] F. V. Kusmartsev, Application of catastrophe theory to molecules and solitons, Phys. Rep. **183**, 1 (1989).
[48] N. Akhmediev, A. Ankiewicz, and R. Grimshaw, Hamiltonian-versus-energy diagrams in soliton theory, Phys. Rev. E **59**, 6088 (1999).
[49] I. H. Malitson, Interspecimen comparison of the refractive index of fused silica, J. Opt. Soc. Am. **55**, 1205 (1965).
[50] A. Couairon, L. Sudrie, M. Franco, B. Prade, and A. Mysyrowicz, Filamentation and damage in fused silica induced by tightly focused femtosecond laser pulses, Phys. Rev. B **71**, 125435 (2005).
[51] A. Couairon and A. Mysyrowicz, Femtosecond filamentation in transparent media, Phys. Rep. **441**, 47 (2007).
[52] C. Milián, A. Jarnac, Y. Brelet, V. Jukna, A. Houard, A. Mysyrowicz, and A. Couairon, Effect of input pulse chirp on nonlinear energy deposition and plasma excitation in water, J. Opt. Soc. Am. B **31**, 2829 (2014).
[53] S. Minardi, C. Milián, D. Majus, A. Gopal, G. Tamosauskas, A. Couairon, T. Pertsch, and A. Dubietis, Energy deposition dynamics of femtosecond pulses in water, Appl. Phys. Lett. **105**, 224104 (2014).
[54] Ge-doped silica is envisaged as a promising platform to make the arrays, because the index contrast Δn, related to the potential depth p, increases slightly with the wavelength and the existence of stable bullets is guaranteed, contrarily to the case of F-doped glass [55]. In the latter case, p is reduced as the bullet's redshift and, hence, the existence of stable bullets becomes compromised [20].
[55] O. V. Butov, K. M. Golant, A. L. Tomashuk, M. J. N. van Stralen, and A. H. E. Breuls, Refractive index dispersion of doped silica for fiber optics, Opt. Commun. **213**, 301 (2002).
[56] http://www.prysmiangroup.com.
[57] D. V. Skryabin and A. V. Gorbach, Colloquium: Looking at a soliton through the prism of optical supercontinuum, Rev. Mod. Phys. **82**, 1287 (2010).
[58] N. Akhmediev, W. Kroikowski, and A. J. Lowery, Influence of the Raman-effect on solitons in optical fibers, Opt. Commun. **131**, 260 (1996).
[59] C. Milián, Y. V. Kartashov, D. V. Skryabin, and L. Torner, Clusters of Cavity Solitons Bounded by Conical Radiation, Phys. Rev. Lett. **121**, 103903 (2018).